

Graphene Q-switched, tunable fiber laser

D. Popa, Z. Sun, T. Hasan, F. Torrisi, F. Wang, and A. C. Ferrari*
Department of Engineering, University of Cambridge, Cambridge CB3 0FA, UK

We demonstrate a wideband-tunable Q-switched fiber laser exploiting a graphene saturable absorber. We get $\sim 2\mu\text{s}$ pulses, tunable between 1522 and 1555nm with up to $\sim 40\text{nJ}$ energy. This is a simple and low-cost light source for metrology, environmental sensing and biomedical diagnostics.

Q-switching and mode-locking are the two main techniques enabling pulsed lasers[1]. In mode-locking, the random phase relation originating from the interference of cavity modes is fixed, resulting in a single pulse[1], with typical duration ranging from tens ps to sub-10 fs[2], and a repetition rate corresponding to the inverse of the cavity round-trip time[2]. In mode-locking, many aspects, including the dispersive and nonlinear properties of the intracavity components, need to be precisely balanced in order to achieve stable operation[1, 2]. Q-switching is a modulation of the quality factor, Q , of a laser cavity[1], Q being the ratio between the energy stored in the active medium and that lost per oscillation cycle[1] (thus, the lower the losses, the higher Q). In Q-switching, the active medium is pumped while lasing is initially prevented by a low Q factor[1]. The stored energy is then released in a pulse with duration ranging from μs to ns when lasing is allowed by a high Q factor[1]. The time needed to replenish the extracted energy between two consecutive pulses is related to the lifetime of the gain medium, which is typically $\sim\text{ms}$ for erbium-doped fibres[1]. Thus the repetition rate of Q-switched lasers is usually low ($\sim\text{kHz}$)[1], much smaller than mode-locked lasers[1, 2]. On the other hand, Q-switching enables much higher pulse energies and durations than mode-locking[1]. Q-switching has advantages in terms of cost, efficient operation (i.e. input power/output pulse energy) and easy implementation, compared to mode-locking, which needs a careful design of the cavity parameters to achieve a balance of dispersion and nonlinearity[1, 2]. Q-switched lasers are ideal for applications where ultrafast pulses ($<1\text{ns}$) are not necessary, or long pulses are advantageous[3, 4], such as material processing, environmental sensing, range finding, medicine and long-pulse nonlinear experiments[3–5].

Q-switching can be active (exploiting, e.g., an acousto-optic or electro-optic modulator[1]), or passive (using, e.g., a saturable absorber (SA)[1]). Passive Q-switching features a more compact geometry and simpler setup compared to active, which requires additional switching electronics[1]. For Q-switching the SA recovery time does not need to be shorter than the cavity round-trip time, since the pulse duration mainly depends on the time needed to deplete the gain after the SA saturates[1, 2], unlike mode-locking[2]. Doped bulk crystals[5], and semiconductor saturable absorber mirrors (SESAMs)[3, 6] are the most common SAs in passive Q-switching[1]. However, the use of doped crystals as SAs requires extra el-

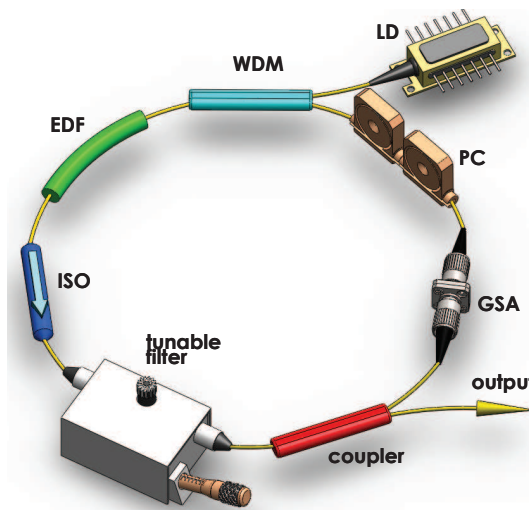


FIG. 1: Setup: laser diode (LD), wavelength division multiplexer (WDM), erbium-doped fiber (EDF), isolator (ISO), graphene SA (GSA), polarization controller (PC)

ements (mirrors, lenses) to focus the fiber output into the crystal[5]. SESAMs have limited operation bandwidth, typically few tens nm[7], thus are not suitable for broad-band tunable pulse generation. Broadband SAs enabling easy integration into an optical fiber system are thus needed to create a compact Q-switched fibre laser.

Single wall carbon nanotubes (SWNTs) and graphene are ideal SAs, due to their low saturation intensity, low cost and easy fabrication[8–22]. Broadband operation is achieved in SWNT using a distribution of tube diameters[8, 17], while this is an intrinsic property of graphene, due to the gapless linear dispersion of Dirac electrons[18–21, 23]. Q-Switching was reported using SWNTs: Ref.24 achieved 14.1nJ pulse energy and $7\mu\text{s}$ width, while Ref.25 13.3nJ and 700ns. After the demonstration of a graphene-based mode-locked laser[17], various group implemented graphene SA in a variety of mode-locked cavity designs[18–22, 26–28].

Here, we demonstrate a fiber laser Q-switched by a graphene saturable absorber (GSA). The broadband absorption of graphene enables Q-switching over a 32nm range, limited only by our tunable filter, not graphene itself. The pulse energy is $\sim 40\text{nJ}$, for $\sim 2\mu\text{s}$ duration.

Graphite flakes are exfoliated by mild ultrasonication with sodium deoxycholate (SDC)[19, 21, 29]. A

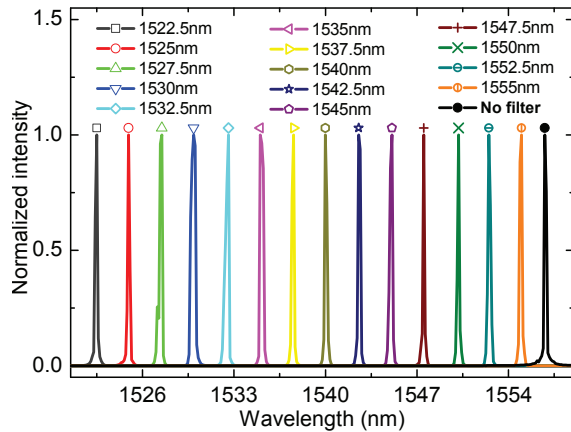


FIG. 2: Output spectra for 14 tuning wavelengths. The curve with a filled circle corresponds to Q-switching without filter.

dispersion enriched with single (SLG) and few layer graphene (FLG)[21] is then mixed with an aqueous solution of polyvinyl alcohol (PVA). After water evaporation, a $\sim 50\mu\text{m}$ thick graphene-PVA composite is obtained[17, 19]. This is then placed between two fiber connectors to form a fiber-compatible SA, then integrated into a laser cavity, Fig.1, with 1.25m erbium doped fiber (EDF) as gain medium, pumped with a 980nm laser diode (LD), coupled via a wavelength division multiplexer (WDM). An optical isolator (ISO) ensures unidirectional light propagation. An in-line tunable optical bandpass filter is inserted after the ISO. Our EDF can support lasing between 1520 and 1560nm[30]. The operation wavelength is selected rotating the dielectric interference filter. The 20% port of an optical coupler provides the laser output. The rest of the cavity consists of a combination of single mode fiber (SMF) Flexcor 1060 and SMF-28. All fibers used in our cavity are polarization-independent, i.e. they support any light polarization, even if this changes as a result of outside perturbations (e.g. mechanical stresses, bending, or temperature). Thus, to improve the output pulse stability, we place in the cavity a polarization controller (PC), consisting of 2 spools of SMF-28 fiber acting as retarders. The total retardation induced by the PC is a function of the fiber geometry in the spool[30]. This allows to maintain a polarization state after each round trip. The total cavity length is $\sim 10.4\text{m}$. The operation is evaluated by a 14GHz bandwidth photo-detector and an oscilloscope. A spectrum analyzer with 0.07nm resolution measures the output spectrum.

Continuous wave (CW) operation starts at $\sim 43\text{mW}$ pump power; pulsed operation at $\sim 74\text{mW}$. The repetition rate is pump-dependent up to $\sim 200\text{mW}$ (Fig.4b), a typical signature of Q-switching[1]. The output spectrum is tunable from ~ 1522 to 1555nm. This is comparable to the 31nm range reported for doped crystal Q-switched tunable lasers[5], but much larger than the 5nm thus far achieved for SWNT Q-switched lasers[24, 25]. Our tun-

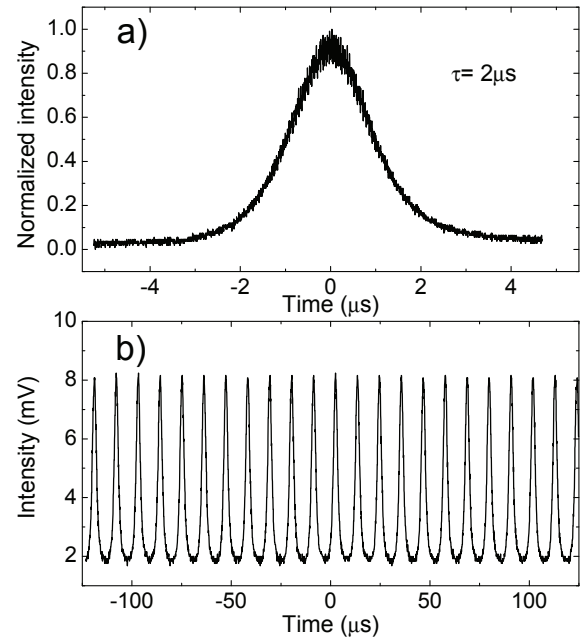


FIG. 3: a) Single pulse envelope. b) Typical pulse train for 2.8mW output power.

ing range is limited by the filter and by the EDF gain, not the GSA. Fig. 2 shows the output spectra for 14 wavelengths at $\sim 2.5\text{mW}$ output power. Without filter, the laser exhibits Q-switching at 1557nm. The full width at half maximum (FWHM) spectral width is $0.3\pm 0.1\text{nm}$ over the whole tuning range, much shorter than thus far achieved for graphene mode-locked lasers[18–22, 26–28].

Fig.3a plots a typical pulse envelope, having $\text{FWHM} \sim 2\mu\text{s}$, comparable to fiber lasers Q-switched with other SAs (e.g. SESAMs[3, 6], doped crystals[5], and SWNTs[24, 25]), but much longer than thus far achieved in graphene mode-locked fiber lasers[18–22, 26–28]. The output pulse duration has little dependence on wavelength, possibly due to the flat gain coefficient of our EDF[30]. Fig.3b shows the pulse train for a typical laser output at 158mW pump power.

The output power varies from 1 to 3.4mW as a function of pump power. The slope efficiency, i.e. the slope of the line obtained by plotting the laser output power against the input pump power[1], is $\sim 2\%$. The repetition rate as a function of pump power varies from 36 to 103KHz (Fig.4b), with a 67KHz change for a 2.4mW output power variation. Unlike mode-locked lasers, where the repetition rate is fixed by the cavity length[1], in Q-switched lasers this depends on pump power[1]. As this increases, more gain is provided to saturate the SA and, since pulse generation relies on saturation, the repetition rate increases with pump power[1]. The maximum output pulse energy is $\sim 40\text{nJ}$ for $\sim 60\text{KHz}$ repetition rate, similar to that achieved using other SAs[25]. Compared to graphene mode-locked fiber lasers[18–22, 26–

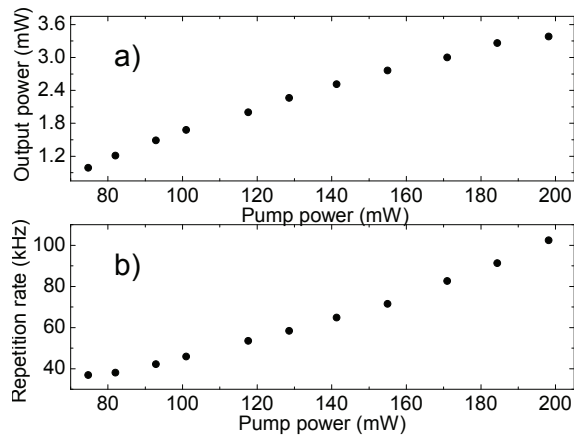


FIG. 4: (a) Output power and (b) repetition rate, as a function of input pump power at 1540nm

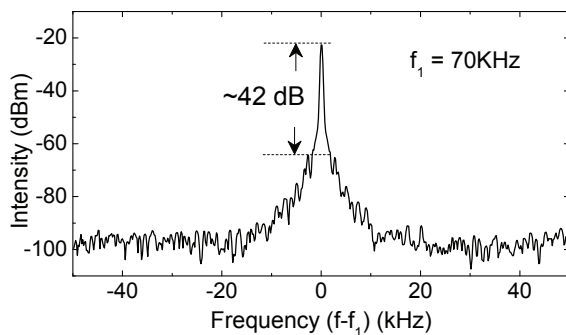


FIG. 5: RF spectrum measured around ~ 70 kHz at 1540nm

28], our pulse energy is ~ 6 times larger, but with less peak power, due to the larger pulse duration. It is also much larger than thus far achieved in SWNT Q-switched lasers [24, 25]. Even higher energies, thus peak powers, could be enabled by evanescent field interaction with GSA [27] and high-gain fibers (e.g. cladding-pumped fibers [5] or large mode area fibers [3]).

The radio-frequency (RF) measurement of the output intensity at 70 Hz, corresponding to a period of $\sim 143 \mu\text{s}$, is shown in Fig. 5. The peak to pedestal extinction is ~ 40 dB (10^4 contrast), confirming pulse stability.

In conclusion, we achieved Q-switching exploiting a graphene-based saturable absorber, using standard, telecom grade, fibre components. The wideband operation of graphene enables broad band tunability. Such wideband Q-switched laser could provide a simple, low-cost, and convenient light source for metrology, environmental sensing and biomedical diagnostics.

We acknowledge funding from EPSRC GR/S97613/01, EP/E500935/1, ERC NANOPOTS, a Royal Society Brian Mercer Award for Innovation, Kings College.

- [1] O. Svelto, *Principles of Lasers*, 4th ed. (Springer, 1998)
- [2] U. Keller, K.J. Weingarten, F.X. Kartner, D. Kopf, B. Braun, I.D. Jung, R. Fluck, C. Honninger, N. Matuschek, J.A. der Au, *IEEE J. Sel. Top. Quant.* **2**, 435 (1996)
- [3] R. Paschotta, R. Häring, E. Gini, H. Melchior, U. Keller, H.L. Offerhaus, D.J. Richardson, *Opt. Lett.* **24**, 388 (1999)
- [4] M. Siniavaeva, M. Siniavsky, V. Pashinin, A. Mamedov, V. Konov, V. Kononenko, *Laser Phys.* **19**, 1056 (2009)
- [5] M. Laroche, A.M. Chardon, J. Nilsson, D.P. Shepherd, W.A. Clarkson, S. Girard, R. Moncorge, *Opt. Lett.* **27**, 1980 (2002)
- [6] S. Kivistö, R. Koskinen, J. Pajaste, S. D. Jackson, M. Guina, O. G. Okhotnikov, *Opt. Expr.* **16**, 22058 (2008)
- [7] O. Okhotnikov, A. Grudinin, M. Pessa, *New J. Phys.* **6**, (2004)
- [8] F. Wang, A.G. Rozhin, V. Scardaci, Z. Sun, F. Henrich, I.H. White, W.I. Milne, A.C. Ferrari, *Nat. Nano.* **3**, 738 (2008)
- [9] S. Y. Set, H. Yaguchi, Y. Tanaka, M. Jablonski, *IEEE J. Sel. Top. Quant.* **10**, 137 (2004)
- [10] A.G. Rozhin, V. Scardaci, F. Wang, F. Henrich, I.H. White, W.I. Milne, A.C. Ferrari, *Phys. Stat. Sol. B* **243**, 3551 (2006)
- [11] A. Martinez, K. Zhou, I. Bennion, S. Yamashita, *Opt. Express.* **18**, 11008 (2010)
- [12] M.A. Solodyankin, E.D. Obraztsova, A.S. Lobach, A.I. Chernov, A.V. Tausenev, V.I. Konov, E.M. Dianov, *Opt. Lett.* **33**, 1336 (2008)
- [13] Z. Sun, A.G. Rozhin, F. Wang, V. Scardaci, W.I. Milne, I.H. White, F. Henrich, A.C. Ferrari, *Appl. Phys. Lett.* **93**, 061114 (2008)
- [14] Z. Sun, T. Hasan, F. Wang, A.G. Rozhin, I.H. White, and A.C. Ferrari, *Nano Res.* **3**, 404 (2010)
- [15] Z. Sun, A.G. Rozhin, F. Wang, T. Hasan, D. Popa, W.O'Neill, A.C. Ferrari, *Appl. Phys. Lett.* **95**, 253102 (2009)
- [16] T.R. Schibli, K. Minoshima, H. Kataura, E. Itoga, N. Minami, S. Kazaoui, K. Miyashita, M. Tokumoto, Y. Sakakibara, *Opt. Express* **13**, 8025 (2005)
- [17] T. Hasan, Z. Sun, F. Wang, F. Bonaccorso, P.H. Tan, A.G. Rozhin, A.C. Ferrari, *Adv. Mater.* **21**, 3874 (2009)
- [18] Z. Sun et al. *Nano Res.* **3**, 653 (2010)
- [19] Z. Sun, T. Hasan, F. Torrisi, D. Popa, G. Privitera, F. Wang, F. Bonaccorso, D.M. Basko, A.C. Ferrari, *ACS Nano* **4**, 803 (2010)
- [20] F. Bonaccorso, Z. Sun, T. Hasan, A.C. Ferrari, *Nat. Photon.* **4**, 611 (2010)
- [21] T. Hasan, F. Torrisi, Z. Sun, D. Popa, V. Nicolosi, G. Privitera, F. Bonaccorso, A.C. Ferrari, *Phys. Stat. Sol. B* (2010)
- [22] D. Popa, Z. Sun, F. Torrisi, T. Hasan, F. Wang, A.C. Ferrari, *Appl. Phys. Lett.* (2010)
- [23] A.K. Geim, K.S. Novoselov, *Nat. Mater.* **6**, 183 (2007)
- [24] D. Zhou, L. Wei, B. Dong, W. Liu, *IEEE Phot. Techn. Lett.* **22**, 9 (2010)
- [25] B. Dong, C. Liaw, J. Hao, J. Hu, *Appl. Opt.* **49**, 5989 (2010)
- [26] H. Zhang, D.Y. Tang, L.M. Zhao, Q.L. Bao, K.P. Loh, *Opt. Expr.* **17**, 17630 (2009)
- [27] Y.W. Song, S.Y. Jang, W.S. Han, M.K. Bae, *Appl. Phys. Lett.* **96**, 051122 (2010)
- [28] A. Martinez, K. Fuse, B. Xu, S. Yamashita, *Opt. Expr.* **18**, 23054 (2010)
- [29] Y. Hernandez et al. *Nature Nano.* **3**, 563 (2008)
- [30] G. Agrawal, *Applications of Nonlinear Fiber Optics*, (Academic Press, 2001)

* Electronic address: acf26@eng.cam.ac.uk